COMBINING MULTI-GNSS FOR PRECISE POSITIONING

C. Deprez, R. Warnant

University of Liège
Quartier Agora
Allée du 6 Août, 19
4000 Liège (Belgium)
Email: cecile.deprez@ulg.ac.be

INTRODUCTION

On 17th November 2016, the Kourou European spaceport, located in French Guiana, will be the theatre of a major step up for the European Global Navigation Satellite System (GNSS) Galileo. Indeed, the European Space Agency (ESA) planed an exceptional fourth-satellites launch thanks to its new Ariane 5 launcher. This operation will bring the number of in–orbit Galileo satellites to 18, event that should enable Initial Operational Capability (IOC) phase to begin by the end of the year leading to initial provision of Galileo operational services.

Similarly to Galileo, the Chinese system BeiDou (BDS), also experienced a prompt expansion. With a 23rd satellite launched on the 12th of June 2016, this constellation, initiated in 1994, is rapidly growing. A full operational system is expected by 2020, which will be composed of five Geostationary Earth Orbit (GEO), three Inclined Geo-Synchronous Orbit (IGSO) and 27 Medium Earth Orbit (MEO) satellites. The signals broadcast by the BDS constellation evolved since the first launch in 2007 and a new generation of satellites is underway. Since 2015, five spacecraft of the BeiDou-3 generation have already reached their orbit and have started broadcasting new B1, B2 and B3 signals, conceived to overlap with the other GNSS frequencies.

To a lesser extent, the American Global Positioning System (GPS) also experienced recent progresses. This system shares, with the two former ones, the common ability of being tracked from Europe and the Code Division Multiple Access (CDMA) technique for signal processing. The GPS modernization started in the early 2000 with the launch of the Block IIR(M) satellite generation including a second civil signal (L2C). The following generation, referred to as Block IIF and launched between 2010 and 2016, brought a third civil signal on L5 frequency. With 12 operational satellites, this latter phase is now completed and the launch of the GPS III generation is expected to begin.

According to [1], the new signal GPS L5, as well as those from the Galileo constellation (E1, E5a, E5b, E5) are all characterized by a high multipath resistance, a low observation noise and an enhanced resistance to interferences. These features might bring a significant improvement in the field of satellite-based positioning and related topics ([2]–[4]). Regarding GPS L5 and Galileo E5a, [5] found evidences that the combination of L5/E5a carrier phases shows better ambiguity resolution performance than the L1/E1 combination, in a single-frequency carrier-phase based positioning. As concerns Galileo E5, it is expected to be revolutionary according to [4], [6], leading to very precise observable precisions, particularly with the code pseudoranges. These improved characteristics are mainly due to its AltBOC modulation ([7]) and its wide bandwidth characteristics ([4]). As a matter of a fact, the composition of this signal, based on the modulation of two sub-carriers E5a and E5b, results in a reference bandwidth of at least 51.150 MHz, corresponding to the largest Radio Navigation Satellite System band ([8]).

In this paper, we first estimated the individual precision of each signal broadcast by the three aforementioned GNSS. For this purpose, we computed single-frequency single-GNSS double difference (DD) combinations between geodetic receivers. We created a short baseline (SB) of approximatively 5 metres, leaving only multipath and observation noise in the positioning equation.

However, even though the Galileo signals would meet the aforementioned great expectations, the influence of the poor geometry of the presently uncomplete satellite constellation degrades the values of precision obtained on position estimations. So far, the increase in Galileo satellite number was not sufficient to solve this issue as it mainly resulted in longer satellite observation periods with a minimum of 4 satellites in view but not in an increase of the number of visible satellites at a single epoch. Therefore, combining Galileo with GPS or BDS appears as a way to solve this issue, as the three systems were designed to be compatible.

Among available frequencies on GPS and Galileo, GPSL1/Galileo E1 and GPSL5/Galileo E5a are overlapping. As far as BDS is concerned, only the B2 signal, emitted by the Phase II BDS satellites, is overlapping the E5b frequency of Galileo. The B1 and B2 signals from the third BDS generation should overlap GPS L1 and Galileo E1 as well as Galileo E5a+b but we could not track them yet. However, because of differences existing between satellite systems, the combined use of overlapping frequencies in real-time dual-GNSS DD induces inter-system biases (ISBs) inside the multi-GNSS equations of observations. Those biases correspond to the differential receiver hardware delays between the constellations forming each pair of overlapping frequencies ([9]). They are introduced by the use of a unique satellite as a pivot for all the constellations in the DD. This technique is known as tight combining, by opposition to the loose combining where a unique pivot satellite is used per constellation ([10], [11]).

With the aim of estimating ISB values for each pair of overlapping frequencies, we computed DD in a zero baseline (ZB) configuration. This configuration, in which receivers are connected to the same antenna by the means of a splitter, achieves the greatest benefit of removing all the errors of the positioning equation with the exception of the receiver noise and the ISB. We conducted this analysis on the L1/E1, L5/B5a and B2 (phase II)/E5b overlapping frequencies. As the ISBs are known to be receiver-dependent, we computed them for each pairs of receivers available at the University of Liège. The equipment we used was composed of two Trimble NetR9, two Septentrio PolaRx4, one PolaRx5 and one PolaRxS connected to two Trimble TRM 59800 SCIS chock ring antennae by the means of a two-way and a four-way splitter. An analysis of their long-term stability was undertaken over years 2014, 2015 and 2016. If identical types of receivers are supposed to show null values of ISBs, receivers from different manufacturers, or even, from the same manufacturer but from a different model, usually show non-negligible values of ISBs ([9], [10]).

Assuming consistent ISB values, the positioning results can be improved by averaging the ISBs over long time spans, and removing them from the DD positioning equation. Therefore, we calibrated the different ISB values obtained with the different receivers/frequencies combinations in order to remove them from the DD positioning equation. We could thus assess the improvement of multi-GNSS on single-GNSS position precisions.

METHODOLOGY

This section describes the methodology used for the evaluation of the observable precisions, the computation of the ISBs and the dual-GNSS improvement assessment on positioning. Those results were computed thanks to a single-frequency relative positioning technique called the double difference. As for the observable precisions, a single-GNSS SB configuration was used while for the ISBs computation, we considered a dual-GNSS ZB configuration. Finally, the dual-GNSS improvement assessment was realized in SB configuration between single-GNSS and dual-GNSS mode.

Computation of the Observable Precisions

Satellite-based positioning relies on time measurement. Indeed, the time required by the signal to travel the satellite-to-receiver distance multiplied by the speed of light results in the distance between the receiver and the satellite. And thus, for a receiver *r,* and a satellite *s*, [12] writes the code pseudoranges and carrier phases single point positioning equation based on a given frequency *j*:

$$R^s_{r,j} = \rho^s_r + c.(dt_r - dt^s) + T^s_r + I^s_{r,j} + M^s_{r,j} + (d_{r,j} - d^s_j) + \varepsilon^s_{r,j} \quad (1)$$

$$\Phi^s_{r,j} = \rho^s_r + c.(dt_r - dt^s) + T^s_r - I^s_{r,j} + m^s_{r,j} + \lambda_j N^s_{r,j} + (\delta_{r,j} - \delta^s_j) + e^s_{r,j} \quad (2)$$

with $R^s_{r,j}$ the code pseudorange observable, $\Phi^s_{r,j}$ the phase pseudorange observable, ρ^s_r the geometric distance between the receiver and the satellite, c the speed of light in the vacuum, dt_r and dt^s the receiver and satellite clock errors and T^s_r the tropospheric delay as the frequency independent terms and $I^s_{r,j}$ the ionospheric delay, $M^s_{r,j}$ the code multipath, $m^s_{r,j}$ the phase multipath, $d_{r,j}$ and d^s_j the receiver and satellite code hardware delays, $\delta_{r,j}$ and δ^s_j the receiver and satellite phase hardware delays, $N^s_{r,j}$ the integer ambiguity term, λ_j the wavelength of the signal and finally, $\varepsilon^s_{r,j}$ and $e^s_{r,j}$ the code and phase observation noises, as the frequency dependent parameters.

Among all those parameters, only the ambiguity and the phase hardware delays are expressed in cycles, the other terms being expressed in metres.

The DD corresponds to the simultaneous observation from two receivers of two common satellites. It consists in the difference between two single differences (SD) that can be themselves defined as differences between simultaneous observations (at time t) from two receivers (1 and 2) of the same satellite *i*:

$$\begin{aligned} R^i_{12,j}(t) &= R^i_{1,j}(t) - R^i_{2,j}(t) \\ &= \rho^i_{12} + c.(dt_1 - dt_2) + T^i_{12} + I^i_{12,j} + M^i_{12,j} + d_{12,j} + \varepsilon^i_{12,j} \end{aligned} \tag{3}$$

$$\begin{aligned} \Phi^i_{12,j}(t) &= \Phi^i_{1,j}(t) - \Phi^i_{2,j}(t) \\ &= \rho^i_{12} + c.(dt_1 - dt_2) + T^i_{12} - I^i_{12,j} + m^i_{12,j} + \lambda_j N^i_{12,j} + \delta_{12,j} + e^i_{12,j} \end{aligned} \tag{4}$$

with $R^i_{12,j}$ the code SD, $\Phi^i_{12,j}$ the phase SD and the indexes $*$ corresponding to the SD terms: $*^i_{12} = *^i_1 - *^i_2$.

This SD combination eliminates the satellite clock dt^s as well as the code and phase hardware delays (d^s_j, δ^s_j) from the equation. When two SD are differentiated into a DD, the codes and phases equations can be written:

$$\begin{aligned} R^{ik}_{12,j}(t) &= R^i_{12,j}(t) - R^k_{12,j}(t) \\ &= \rho^{ik}_{12} + T^{ik}_{12} + I^{ik}_{12,j} + M^{ik}_{12,j} + \varepsilon^{ik}_{12,j} \end{aligned} \tag{5}$$

$$\begin{aligned} \Phi^{ik}_{12,j}(t) &= \Phi^i_{12,j}(t) - \Phi^k_{12,j}(t) \\ &= \rho^{ik}_{12} + T^{ik}_{12} - I^{ik}_{12,j} + m^{ik}_{12,j} + \lambda_j N^{ik}_{12,j} + e^{ik}_{12,j} \end{aligned} \tag{6}$$

with $R^k_{12,j}$ the code SD on satellite *k*, $R^{ik}_{12,j}$ the code DD, $\Phi^k_{12,j}$ the phase SD on satellite *k*, $\Phi^{ik}_{12,j}$ the phase DD and the indexes $*^{ik}_{12}$ corresponding to the DD terms: $*^{ik}_{12} = *^i_{12} - *^k_{12}$.

The DD presents the advantage of completely removing the satellite and receiver clock errors as well as the satellite and receiver hardware delays. Moreover, depending on the relative positions of the two receivers, some other parameters can also be removed from the equation. If the baseline length between the two receivers is very short (a few metres as it is the case in our experiment), the atmospheric errors (T^{ik}_{12} and $I^{ik}_{12,j}$) can be neglected as the SD atmospheric errors are identical for each receivers on these short distances. With such configurations of the receivers, the only errors remaining in the DD code pseudorange equation are the multipath and the observation noise, to which can be added the integer ambiguity in the case of the phase DD equation. Neglecting the multipath influence, the observation noise can be estimated thanks to this configuration and the observable precisions computed on this basis.

In relative positioning, the SD and DD observable precisions (σ_{SD} and σ_{DD}) can be obtained from individual one way observable precisions (σ_1 for the observations made at receiver 1 and σ_2 for those made the receiver 2), and vice versa. The observations used to form SD and DD being independent, we can write:

$$\sigma^2_{SD} = \sigma^2_1 + \sigma^2_2 \tag{7}$$

$$\sigma^2_{DD} = 2.\sigma^2_1 + 2.\sigma^2_2 \tag{8}$$

If receivers 1 and 2 are both identical and from the same manufacturer, their individual observable precisions will also be identical. And therefore:

$$\sigma_{DD}^2 = 4.\sigma_1^2 \tag{9}$$

In practice, we used this formula to estimate the individual observable precisions from the DD precisions. As we neglected the multipath in this equation, we might over-estimate the individual observable precisions.

Computation of the ISBs

Formulas from the above section have been written for a single-GNSS model. When a dual-GNSS system is considered, few more considerations have to be taken into account. Indeed, if the Galileo, GPS and BDS systems are sharing similar frequencies, thus being compatible, they still present intrinsic differences. Each system has its own reference time, into which satellites broadcast information are given (orbit and clock), and therefore, a corrective term needs to be inserted in the Galileo single point positioning equation when combined with GPS so that the information broadcast by the Galileo satellites in the Galileo reference time are now given in the GPS reference time. This term is called the Galileo to GPS Time Offset (GGTO). If the satellite from GPS is noted *G*, the one from Galileo noted *E*, and that they are simultaneously observed by a receiver *r*, the single point positioning carrier phase (*in a similar way*: code pseudorange) equation of Galileo becomes:

$$\Phi_{r,j}^E = \rho_r^E + c.(dt_r - dt^E - GGTO) + T_r^E - I_{r,j}^E + m_{r,j}^E + \lambda_j N_{r,j}^E + (\delta_{r,j}^{(E)} - \delta_j^E) + e_{r,j}^E \tag{10}$$

In a SD configuration though, this terms disappears:

$$\Phi_{12,j}^E = \rho_{12}^E + c.(dt_1 - dt_2) + T_{12}^E - I_{12,j}^E + m_{12,j}^E + \lambda_j N_{12,j}^E + \delta_{12,j}^{(E)} + e_{12,j}^E \tag{11}$$

Still, a differential term, which was eliminated in the single-GNSS DD model, remains in the dual-GNSS DD: the differential receiver hardware delay between the two constellations. In a ZB configuration, the DD do not contain any influence of the atmospheric errors, the multipath as well as the observation noise before the splitter and we can therefore write for carrier phases (*in a similar way*: code pseudoranges):

$$\Phi_{12,j}^{GE} = \rho_{12}^{GE} + \lambda_j N_{12,j}^{GE} + \delta_{12,j}^{(GE)} + e_{12,j}^{GE} \tag{12}$$

This differential receiver hardware delay between GPS and Galileo is referred to as inter-system bias. It appears only when combinations of mixed-GNSS satellites are computed in a tight combing DD. The code ISBs are estimated as an additional unknown in a least square adjustment together with the position unknowns (X, Y, Z). The method is different when it comes to carrier phase ISBs, the entire part of the ISBs being estimated all together with the integer ambiguity thanks to the LAMBDA method ([13]), so that only the fractional part (between -0.5 and 0.5 cycles) remains to be estimated as an additional error. In this study, we compared our epoch-by-epoch code ISB results with 10-minutes average ISBs to observe their variability over short time spans and getting rid of individual epoch errors. However, with the carrier phase data, we only considered an epoch-by-epoch resolution in order to avoid cycle slips, the results begin independent from one epoch to the other.

Computation of the Position Precisions

Once the averaged ISB values were estimated for each pairs of receivers, we removed them from the DD position equation. By reducing the number of unknowns from four to three, the redundancy of the observations is increasing, which should engender, as a result, an improvement of the precision on position estimations. Finally, we compared single-GNSS DD to dual-GNSS DD in SB configuration in order to estimate the improvement resulting from the addition of a new constellation to the equation.

RESULTS

Observable Precisions

Based on the methodology detailed in the previous section, we computed GPS, Galileo and BDS observable precisions. These results are available from Table 1, 2 and 3. We computed an average value of the observable precision of each GPS, Galileo and BDS signal on the basis of a consecutive 10-days period analysis in 2016 (Days of Year (DOYs) 145 to 154). During this period, a SB of approximatively 5 metres between identical receivers (two Trimble NetR9 and two Septentrio X4) was set up at Liège. We used precise ephemeris data to compute the satellite orbits in order to limit the errors due to the orbit estimation. As an additional precaution and given their specific orbit, we did not consider the E14 and E18 satellites of the Galileo constellation. Besides, the E20 satellite was also rejected from computation as it has been declared unhealthy. As regards the BDS constellation, we computed our precision values without considering the very recent phase III satellites. An epoch-by-epoch solution was computed on 30 seconds datasets for each of the 10 days, and the precision values were weighted by the duration of the observation periods of satellites. We had the receiver position precisely fixed so that no error coming from an a priori position estimation could influence our results. We also considered a 10 degrees elevation mask to avoid low altitude satellites to degrade to solution.

Regarding the type of receiver, some clarifications should be made concerning the notations used in this paper and the RINEX format naming. If for GPS and BDS, the L1, L2, L5, B1, B2 and B3 signals refer to the C1C/L1C, C2W/L2W, C5Q/L5Q, C1I/L1I, C7I/L7I, C6I/L6I RINEX nomenclature for codes and phases on both Septentrio and Trimble receivers, for Galileo, only the quadrature component (-Q) of the signals is tracked by the Septentrio receivers while the Trimble receivers are able to track both I+Q components of the signals.

From Tables 1, 2 and 3, it appears that the Galileo signals show the best precision values as far as code pseudoranges are concerned. Particularly, Galileo E5 AltBOC outperforms all the other signals. These results meet the expectations detailed in the Introduction section. We can also notice that, if the two different types of receivers show different values of precisions, they both draw to identical conclusions. Furthermore, as expected, the GPS L5 signal shows values of precisions very close to GPS L2, but far better than GPS L1. Indeed, among GPS and Galileo signals, L1 and E1 present the worse values of precisions. Regarding BDS signals, if their precisions are far from reaching those of the Galileo signals, they are close to the GPS signal ones, even if less good.

Inter-System Biases

We computed epoch-by-epoch ISBs for both codes and phases, thanks to a least square adjustment, using fixed precise coordinates for each antenna as a priori values for the receiver positions. We conducted the analysis of the ISBs over 2014, 2015, 2016 in order to observe their evolution over long time spans. For the year 2014, data from DOYs 345 to 355 were collected for same manufacturer receiver ISBs computation. During this period, the Septentrio X4 and Septentrio XS receivers were configured in a ZB as well as the two Trimble NetR9. This configuration was reversed for the DOYs 310 to 320 during which the mixed-receivers ISBs were computed. In 2015, two mixed-receivers ZB were configured between DOYs 190 and 200, between our Trimble NetR9 and our Septentrio X4 and XS. The identical-receivers ZB were computed over DOYs 330-340 for this same year. Finally, in 2016, we considered two different periods of observation for the mixed-receivers ZB. One from DOYs 13-166, where a third ZB was tested between Trimble Net R9 and Septentrio X5, and one between DOYs 167-212 of 2016. Indeed, the activation of the Trimble receiver multipath filter on DOY 167 impacted to a large extent the ISB values. The identical-receiver ZB was computed during the early 2016 (DOYs 1 to 12).

Table 1. Precisions of the GPS signals (metres)

RECEIVER		L1	L2	L5
Septentrio	Codes	0.20	0.12	0.14
	Phases	0.0013	0.0016	0.0014
Trimble	Codes	0.38	0.31	0.30
	Phases	0.0018	0.0023	0.0021

Table 2. Precisions of the Galileo signals (metres)

RECEIVER		E1	E5a	E5b	E5
Septentrio	Codes	0.17	0.14	0.014	0.06
	Phases	0.0015	0.0020	0.0019	0.0018
Trimble	Codes	0.24	0.22	0.24	0.14
	Phases	0.0021	0.0021	0.0023	0.0022

Table 3. Precisions of the BDS signals (metres)

RECEIVER		B1	B2	B3
Septentrio	Codes	0.33	0.25	-
	Phases	0.0015	0.0019	-
Trimble	Codes	0.41	0.31	0.26
	Phases	0.0023	0.0026	0.0024

According to [10] and [9], identical-pairs of receivers should lead to zero values of ISBs while mixed-pairs should not. In both cases, these studies observed very stable code ISBs. Averaged code ISB results for the first part of 2016 are presented in Tables 4, 5, 6. From this Tables, only the Septentrio identical-receiver pairs lead to zero values with all the overlapping frequencies tested. Indeed, the Trimble-Trimble pairs, in the case of Galileo E5b/BDS B2 and GPS L1/Galileo E1 show unexpected non-zero ISBs. Therefore, we conducted a detailed analysis of the L1/E1 pair over years 2015 and 2016. In Fig. 1, one can observe than the ISBs between the Trimble receivers are not stable over time. To identify the source of this instability, we combined those two Trimble receivers with a Septentrio X4 and one of them (Trimble 1) revealed a significant instability over time (Fig. 2). This evolution, not influenced by the firmware updates of the receivers, might be due to temperature changes inside the receiver room. In Fig. 3, a graph of the temperature along year 2015 is presented and its evolution seems to be correlated to the ISBs behaviour. However, the non-zero value observed on the E5b/B2 pair does not seem to suffer from any evolution, showing a stable non-zero value over time. Regarding the pairs formed by the different models of Septentrio receivers, their values are very close to zero, and can be neglected except for E1/L1 pair. The mixed-receiver ISB values are not negligible as they can even reach more than 4 metres on L5/E5a. Their evolution over the 2014, 2015 and 2016 studied periods is rather stable, expect for the L1/E1 ISBs computed with Trimble 1.

Since DOY 166, the Trimble receiver multipath filter was turned on, leading to important changes in the ISB code results (see Tables 7, 8 and 9) for two overlapping frequencies out of three (L5/E5a and L1/E1). In contrast, the Septentrio receiver multipath filter activation and deactivation did not cause any significant modification of the ISB values.

As a conclusion, it appears that firmware updates of the receivers do not show influence on code ISBs with our receiver set during our study periods but the activation of the multipath filter of some receivers does. Moreover, if we could not demonstrate a clear influence of receiver temperature variations on ISBs, it seems that some receivers are less stable than others. And this instability needs to be taken into account with the aim of achieving proper ISB corrections for position estimations. Finally, the 10-minutes analysis conducted in parallel of the epoch-by-epoch one confirmed the Tables 4, 5, 6, 7, 8 and 9 results.

Similarly to the code analysis, we conducted a phase ISB assessment. Over identical periods of study as for code ISBs, we were not able to detect any influence of the receiver firmware updates. As for the L1/E1 and L5/E5a phase ISBs, they presented close to zero results in both identical and mixed-receiver pairs. The E5b/B2 overlapping frequencies showed null ISB values for identical-receiver pairs and non-null ISB values for mixed-receiver pairs. However, we could not observe, on any of these phase ISBs, the variability observed with the codes on L1/E1. Finally, the activation of Trimble and Septentrio multipath mitigation filters did not show any influence on phase ISBs.

Table 4. Averaged GPS L5/Galileo E5a code ISBs (metres)

	TR	**X4**	**XS**	**X5**
TR	0.00	-4.44	-4.49	-4.48
X4	4.44	0.00	-0.04	-0.03
XS	4.49	0.04	-	-0.02
X5	4.48	0.03	0.02	-

Table 5. Averaged Galileo E5b/BDS B2 code ISBs (metres)

	TR	**X4**	**XS**
TR	0.13	-2.82	-2.57
X4	2.82	0.02	-0.04
XS	2.57	0.04	-

Table 6. Averaged GPS L1/Galileo E1 code ISBs (metres)

	TR	**X4**	**XS**	**X5**
TR	0.15	-0.22	-0.16	-0.02
X4	0.22	0.00	-0.00	-0.17
XS	0.16	0.00	-	-0.17
X5	0.02	0.17	0.017	-

Table 7. Averaged GPS L5/Galileo E5a code ISBs (metres) after Trimble multipath filter activation

	TR	**X4**	**XS**	**X5**
TR	-	-5.98	-6.03	-6.03
X4	5.98	-	-0.05	-0.04
XS	6.03	0.05	-	-0.01
X5	6.03	0.04	0.01	-

Table 8. Averaged Galileo E5b/BDS B2 code ISBs (metres) after Trimble multipath filter activation

	TR	**X4**	**XS**
TR	-	-2.87	-2.57
X4	2.87	-	-0.04
XS	2.57	0.04	-

Table 9. Averaged GPS L1/Galileo E1 code ISBs (metres) after Trimble multipath filter activation

	TR	**X4**	**XS**	**X5**
TR	-	-1.62	-1.65	-1.80
X4	1.62	-	-0.00	-0.17
XS	1.65	0.00	-	-0.17
X5	1.80	0.17	0.17	-

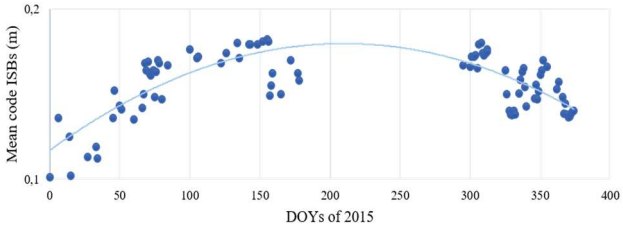

Fig 1. Trimble ZB and SB code ISBs analysis (year 2015)

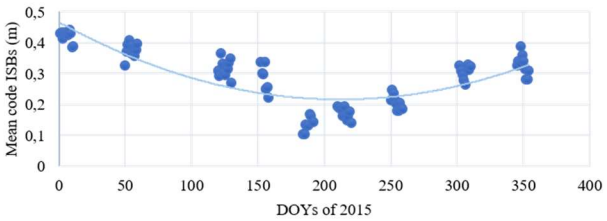

Fig 2. TR 1 and Sept X4 ZB code ISBs analysis (2015)

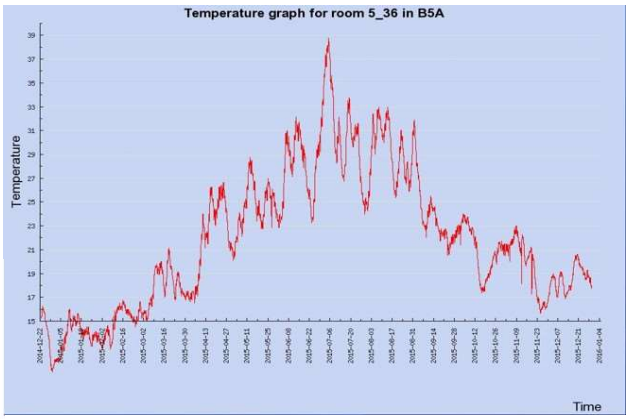

Fig 3. Temperature inside the receivers room over year 2015 (°C)

Position Precisions

In L5/E5a and E5b/B2 cases, we computed averaged values of both code and phase ISBs as they were stable over time. Regarding L1/E1, the variability of our code ISB solution needed to be considered for a precise correction. Therefore, we created a routine averaging the 5-previous days' code ISB values and then using this mean value as an ISB correction. From Fig. 4, the comparison between non-estimated (positioning equation non-corrected and no estimation of the ISBs), estimated (positioning equation non-corrected and estimation of the ISBs as an additional unknown) and corrected (positioning equation corrected with an average ISB value) code ISB positioning cases is illustrated for the L5/E5a combination in a ZB mixed-receivers (Trimble – Septentrio X4) configuration. It obviously appears that removing the ISBs from the DD positioning equation allow reaching more precise baseline precision as only the three positioning unknowns remain to be determined. Indeed, the uncorrected baseline precision value reached 8.11 metres whereas the estimated baseline precision only reached 1.60 metres and that a final precision of 1 metre was obtained when the averaged ISB value was removed from the ZB DD positioning equation. This experiment was conducted on DOYs 88 to 96 of 2016.

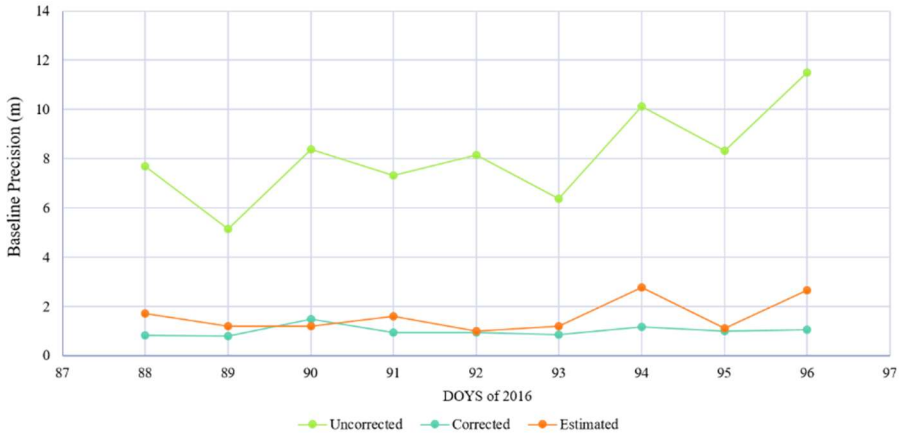

Fig 4. Baseline precisions of Trimble and Septentrio X4 receivers in a ZB configuration (metres)

Regarding the comparison between the position precisions of single-GNSS and dual-GNSS SB DD, we observed a real improvement when combining Galileo with GPS and BeiDou. Indeed, due to a poor geometry, the reduced constellation of Galileo highly degrades the positioning, implying high Position Dilution of Precision (PDOP) values. Using a dual-GNSS system avoid these rise of the PDOP, and therefore, increase the quality of positioning. But, the excellent quality of the Galileo signals, studied in the first subsection, being combined with another signal, is degraded. Nonetheless, the improvement brought by the higher number of satellite available for positioning compensates it.

CONCLUSION

A first analysis of the quality of GPS, Galileo and BDS signals revealed high precision positioning potential for newly available signals (GPS L5 and Galileo E1/E5a/E5b/E5). Indeed, using a 10 degrees elevation mask, we found particularly promising precisions with Galileo, ranging from 5 to 17 centimetres on code pseudoranges, and GPS, with values from 2 to 20 centimetres, while the BDS observables only reached 26 to 40 centimetres on the position precisions. However, the number of satellites broadcasting such frequencies being limited, the potential of those signal cannot be exploited yet. Indeed, the geometry PDOP factor reaches very elevated values, which degrades the positioning solutions using those signals. Therefore, combining the GNSS appears as an opportunity to compute precise positions with low PDOP values. But, due to differences between GNSS, ISBs must be estimated as a fourth unknown in the positioning equation. A long-term analysis of L1/E1, L5/E5a, E5b/B2 ISBs revealed a good stability over time, excepted for a particular receiver on the L1/E1 frequency. Nonetheless, an attempt for retrieving averaged values of ISBs from positioning equation revealed an improvement of 40 centimetres on the position precision. It was finally observed that dual-GNSS improved the single-GNSS SB DD positioning.

REFERENCES

[1] O. Julien, J.-L. Issler, L. Lestarquit, and L. Ries, “Estimating the Ionospheric Delay Using GPS/Galileo Signals in the E5 Band,” *Inside GNSS*, vol. 10, no. 2, pp. 54–64, Apr. 2015.

[2] P. F. de Bakker, C. C. J. M. Tiberius, H. van der Marel, and R. J. P. van Bree, “Short and zero baseline analysis of GPS L1 C/A, L5Q, GIOVE E1B, and E5aQ signals,” *GPS Solutions*, vol. 16, no. 1, pp. 53–64, Jan. 2012.

[3] P. F. Silva *et al.*, “Results of Galileo AltBOC for precise positioning,” in *Satellite Navigation Technologies and European Workshop on GNSS Signals and Signal Processing,(NAVITEC), 2012 6th ESA Workshop on*, 2012, pp. 1–9.

[4] T. Diessongo, T. Schüler, and S. Junker, “Precise position determination using a Galileo E5 single-frequency receiver,” *GPS Solutions*, vol. 18, no. 1, pp. 73–83, 2014.

[5] N. Nadarajah, A. Khodabandeh, and P. J. G. Teunissen, “Assessing the IRNSS L5-signal in combination with GPS, Galileo, and QZSS L5/E5a-signals for positioning and navigation,” *GPS Solutions*, vol. 20, no. 2, pp. 289–297, Apr. 2016.

[6] I. Colomina *et al.*, “Galileo’s Surveying Potential: E5 Pseudorange Precision,” *GPS World*, vol. 23, no. 3, pp. 18–33, Mar. 2012.

[7] N. C. Shivaramaiah and A. G. Dempster, “The Galileo E5 AltBOC: understanding the signal structure,” in *International Global Navigation Satellite Systems Society, IGNSS Symposium, Qld, Australia*, 2009, pp. 1–3.

[8] O. Julien, L. Priya, J.-L. Issler, and L. Lestarquit, “Estimating the Ionospheric Delay Using GPS/Galileo Signals in the E5 Band,” in *EWGNSS 2013, 6th European Workshop on GNSS Signals and Signal Processing*.

[9] D. Odijk and P. J. G. Teunissen, “Characterization of between-receiver GPS-Galileo inter-system biases and their effect on mixed ambiguity resolution,” *GPS Solutions*, vol. 17, no. 4, pp. 521–533, Oct. 2013.

[10] J. Paziewski and P. Wielgosz, “Accounting for Galileo–GPS inter-system biases in precise satellite positioning,” *Journal of Geodesy*, vol. 89, no. 1, pp. 81–93, Jan. 2015.

[11] O. Julien, P. Alves, E. M. Cannon, and G. Lachapelle, “Improved triple-frequency GPS/Galileo carrier phase ambiguity resolution using a stochastic ionosphere modeling,” presented at the ION NTM, San Diego, CA, 2004, p. 12.

[12] J. Sanz Subirana, J. M. Juan Zornoza, and M. Hernández-Pajares, *Fundamentals and algorithms. Vol. 1. Vol. 1.* Noordwijk: ESA Communications, 2013.

[13] P. J. Teunissen, “The least-squares ambiguity decorrelation adjustment: a method for fast GPS integer ambiguity estimation,” *Journal of geodesy*, vol. 70, no. 1–2, pp. 65–82, 1995.